"A Cochlear Nucleus Auditory prosthesis based on microstimulation"

Contract No. **No. NO1-DC-4-0005**
Progress Report #6

HUNTINGTON MEDICAL RESEARCH INSTITUTES
NEURAL ENGINEERING LABORATORY
734 Fairmount Avenue
Pasadena, California 91105

D.B. McCreery, Ph.D.
L.A. Bullara, B.S.
A.S. Lossinsky, Ph.D.

HOUSE EAR INSTITUTE
2100 WEST THIRD STREET
Los Angeles, California 90057

R.V. Shannon Ph.D
S. Otto M.S.
M. Waring, Ph.D

SUMMARY

One goal of this project is to develop arrays of multisite silicon-substrate electrodes, which should allow placement of many more microstimulating sites within the human cochlear nucleus than is possible with discrete iridium microelectrodes. We are developing and evaluating arrays that have 16 electrode sites distributed along 4 silicon shanks extending from an epoxy superstructure that is 2.4 mm in diameter.

In the last quarter, we continued our evaluations of the capabilities of these silicon substrate arrays implanted chronically in the cochlear nucleus of young adult cats. Here we report data from a terminal experiment conducted in a cat in which the microstimulating array had been implanted in the cochlear nucleus for 250 days. Response growth functions of the compound response evoked by the microstimulation in the cochlear nucleus were recorded via an electrode implanted chronically near the rostro-medial pole of the contralateral inferior colliculus. The thresholds and growth with stimulus amplitude were quite stable between the 22nd and 250th day after array implantation, but there were indications of some ongoing movement of the silicon shanks through the tissue, and this was confirmed at autopsy. The slow subsidence of the array in cat 153 and the more extensive dislocation of the array in cat 149 probably can be attributed to our method of routing of the array cable, which has subsequently been redesigned.

In cat 153 we continued our evaluation of the capacity of the intranuclear microstimulating arrays to access separate neuronal population over a range of stimulus amplitudes. Multiunit neuronal activity was recorded in the central nucleus of the contralateral ICC using a 32-site silicon substrate probe. We generated post-stimulus time (PST) histograms of the neuronal activity that was recorded at each of 16 sites in the ICC and then generated contour ("topographic") maps of the evoked neuronal activity from the set of 16 PST histograms. Even at the highest stimulus amplitude used (30 μA) adjacent microstimulating sites in the medial part of the CN separated by only 300 μm induced neuronal activity in largely non-overlapping regions along the dorsolateral-ventromedial axis ICC. Particularly for the probe shanks in the caudal part of the posteroventral cochlear nucleus, the ordering of the depths of the centroids of activity induced in the central nucleus of the IC corresponded precisely to the tonotopic organization of the cochlear nucleus. Overall, the sites on the two shanks in the caudal part of the PVCN, rostral of the octopus cell region, spanned the greatest range of acoustic frequency, from above 25 Khz to approximately 1 Khz.

Since the human and feline ventral cochlear nuclei contain similar cell types and the nuclei or both species are of similar size and structure, these data demonstrate the potential for a central auditory prosthesis using multisite silicon-substrate probes, and suggests the number and density of shanks and individual stimulating sites that will be necessary to access the entire tonotopic gradient of the human ventral CN.

On Dec 13, 2005 , the 6th patient was implanted with an array of macroelectrodes in the lateral recess and the array of penetrating microelectrodes. This hybrid implant is designated the penetrating ABI (PABI). PABI patient #6 received the new revised model of the penetrating array with 10 stimulating sites, each with increased surface area (8,000 μm^2) to allow use of a greater charge range. The implant's device was activated on Jan 15, 2006. The patient was unable to use the surface array due to intolerable non-auditory side effects but 6 of the microelectrodes on the penetrating array provided auditory percepts over a full range of loudness without side effects. Data from this patient will be presented in the next quarterly report.

In a testing session in December 2005, in Verona, Italy, data were obtained on temporal integration and thresholds of auditory percepts as a function of stimulus pulse phase duration, from 9 patients with the surface type of auditory brains implants (ABI's). The first patient with a surface ABI device placed on the Inferior Colliculus (called the Inferior Colliculus Implant - ICI) also was tested. For most of these patients, their deafness was of etiologies other than Type 2 Neurofibromatosis (NF2) and some had high levels of speech recognition with the ABI. Testing focused on temporal measures on the hypothesis that speech recognition and temporal resolution were linked. Previous test results show a significant correlation between speech recognition and temporal modulation detection levels.

1: Work completed at HMRI

Evaluation of a multi-site silicon-substrate microstimulating array

INTRODUCTION

The workscope of our contract calls for the development of arrays of silicon substrate electrodes, which should allow placement of many more electrode sites into the human cochlear nucleus than is possible with discrete iridium microelectrodes. We are developing arrays for implantation into the human cochlear nucleus that have 16 electrode sites distributed on 4 silicon shanks extending from an epoxy superstructure that is 2.4 mm in diameter. We have been conducting animal studies using microstimulating arrays with silicon substrate probes fabricated at the University of Michigan under the direction of Design Engineer Jamille Hetke. Figure 1A shows a probe with 2 shanks and 8 stimulating sites, that have been sputter-coated with iridium oxide. The 4 sites on each shank are 0.8mm to 1.7 mm below the top of the shanks. Figure 1B shows an array containing 2 of the probes (4 shanks and 16 electrode sites) extending from an epoxy superstructure that floats of the surface of the cochlear nucleus. The cable is angled vertically, to accommodate the trans-cerebellar approach to the feline cochlear nucleus.

In principle, the silicon substrate array could provide improve functionality of a central auditory prosthesis by affording highly localized stimulation of neuronal populations within the ventral cochlear nucleus (VCN). This localized stimulation should allow precise and selective access to the tonotopic

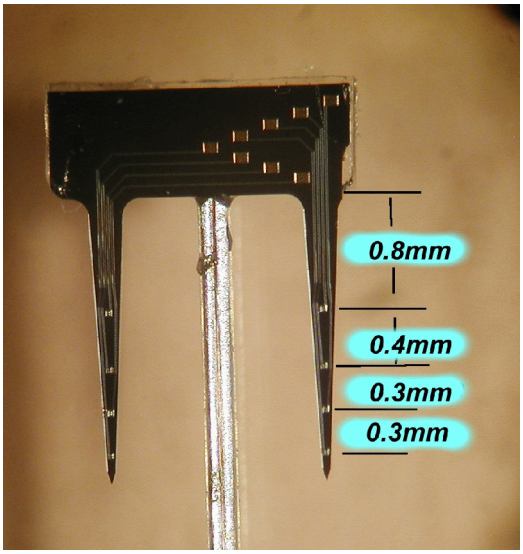

Figure 1A

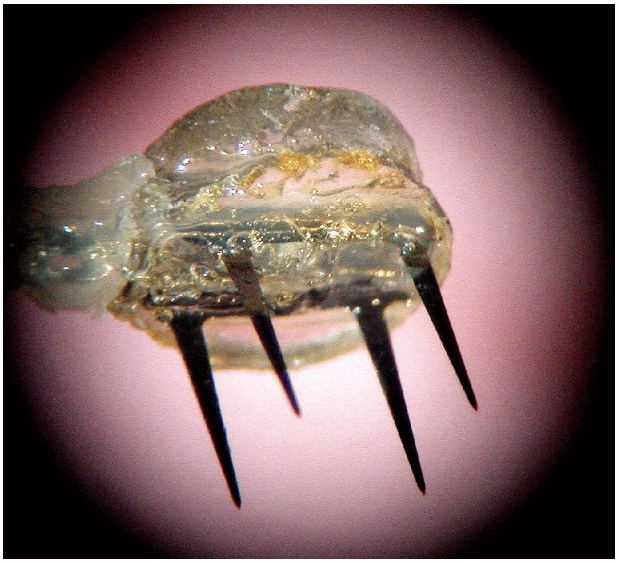
Figure 1B

organization within each of the subdivisions of the cochlear nucleus (CN), but intranuclear microstimulation will excite the axonal projections from the CN as well as the cell bodies, and also may depolarize the large dendrites that may span auditory nerve terminal representing a range of acoustic frequencies.

In previous reports, we have described a method of quantifying the ability of the intranuclear microstimulation to selectively activate the tonotopic organization of the lower auditory system, using current source-sink density analysis of the evoked responses recorded in the contralateral inferior colliculus. The tonotopic organization of the anteroventral and posteroventral CN is preserved in the projection from the CN to the inferior colliculus. The iso-frequency laminae are oriented more-or-less perpendicular to the dorsolateral-venteromedial axis of the central nucleus of the inferior colliculus (ICC) with lower acoustic frequencies represented dorsally and high frequencies represented ventrally and medially (e.g. Semple and Aitkins, 1979, Brown et al, 1997).In this report, we present results from a cat in which the microstimulating

array was implanted for 250 days.

METHODS

Array implantation

Microstimulating arrays are implanted chronically into the cochlear nucleus of your adult cats. Using aseptic technique, the scalp is opened in a midline incision, and the muscles reflected. A small craniectomy is made over the right occipital cortex and the bipolar recording electrode introduced into the rostral pole of the rleft inferior colliculus. The reference electrode was dorsal to the colliculus. These electrodes are solid 100 µm ss wire, with ~ 1 mm of the Teflon insulation removed for the tips.

To access the cochlear nucleus, a craniectomy is made over the right cerebellum, extending up to the tentorium. The rostrolateral portion of the left cerebellum is aspirated using glass pipettes. The electrode array is secured on the end of a vacuum wand, and thereby advanced into the cochlear nucleus. Before releasing the vacuum, the array cable is fixed to the bone at the margin of the craniectomy, using medical grade SuperGlue and the cavity was filled with gelfoam.

Recording of evoked responses

Periodically, the responses evoked from each of the microelectrodes in the left cochlear nucleus were recorded via the electrode in the rostral pole of the right inferior colliculus. The stimulus was cathodic-first, charge-balanced pulse pairs, each phase 150 µs in duration, ranging from 0 to 35 µA in amplitude. 512 to 2048 successive responses were averaged to obtain each averaged evoked response (AER). The response growth functions, which represent the recruitment of the neural elements surrounding the microelectrode, were generated for each stimulating electrode site in the PVCN, by plotting the amplitude of the first component of each of the AERs evoked from that site, against the amplitude of the “probe” stimulus that evoked the AER.

Multisite recording in the inferior colliculus

This terminal experiment was performed immediately before the cat was sacrificed. The procedure is essentially as described in our previous quarterly reports (QPR #4,5). The cat wae anesthetized with Isoflurane and nitrous oxide, its heads fixed in a stereotaxic holder with hollow ear bars, to facilitate the delivery of acoustic stimuli. A wide craniectomy was made over the left posterior cerebral hemisphere, and the occipital pole of the cerebrum was removed by aspiration to expose the inferior colliculus. The cat was transported to a double-walled acoustic isolation room with its head still fixed in the stereotaxic holder. Throughout the remainder of the experiment, anesthesia was maintained with a mixture of 2-2.5% Isoflurane and oxygen delivered by a self-breathing apparatus. Respiration rate and end-tidal CO_2 was monitored continuously. Core body temperature was maintained at 37-39.0˚C using a circulating water heating pad. All sound-generating support equipment was located outside of the sound isolation room.

Microstimulation was applied in the cochlear nculeus via the chronically-implanted array. Multiunit neuronal activity was recorded in the contralateral inferior colliculus using a 32-site silicon substrate probe designed and fabricated by NeuroNexus, Inc., and modifed at HMRI to reduce bucking as their tips are pressed against the pia overlying the IC. The recording sites are spaced 100 µm apart over a total span of 3 mm, which is somewhat less than the span of the domestic cat’s ICC along the dorsolateral-ventromedial axis (approximately 4.5 mm). The recording probe was inserted into the inferior colliculus at an angle of 45º from the vertical, and approximately along the tonotopic gradient.

For each penetration of the recording probe into the ICC, the response to acoustic stimuli was recorded in the ICC. Tone bursts spanning 2.6 to 26 KHz (approximately 80 db spl, and 100 ms in duration with a rise time of 10 ms) were used. Neuronal activity was recorded simultaneously from alternate probe sites (16 sites, spaced 200 µm apart) using the custom hardware and computer software described in previous progress reports. Then, controlled-current, biphasic stimulus pulses (150 µs/ph in duration at 50 Hz) were applied to the individual microelectrode sites in the cochlear nucleus. 1500 successive stimulus pulses were delivered in sequence at 50 hz through each microstimulating sites in the CN. The stimulus

current was 10, 20 and 30 μA (1.5, 3 and 4.5 nC/phase). In the human patients implanted to date, the thresholds for auditory percepts from the penetrating microelectrodes have been 1.7 nC/phase or less .

Data were analyzed offline used the custom software described in previous reports. First, a common template of the compound evoked responses is generated by summing (averaging) 1500 successive responses to the microstimulation. This template then is subtracted from each individual trace (response), in order to suppress the large evoked response. Low- and high-frequency noise that is unique to each trace then is removed by broadband filtering using a passband of 1000-8000 Hz (time domain convolution filter using sinx/x kernels).

Neuronal action potentials (multi-unit activity) were detected as events that exceeded 3.5 x the rms noise level of the recordings. Post-stimulus time (pst) histograms were generated from those events. Contour ("topographic style") maps of the evoked neuronal activity were generated from the set of 16 PST histograms representing the neuronal activity recorded along the dorsolateral-ventromedial axis if the ICC. On these contour maps, the ordinate is the distance above the deepest recording site in the ICC (at the tip of the probe), and the abscissa is time after the stimulus pulse. The contour line labels represent the total number of action potentials in each of the 100 μs bins of the PST histograms from which the maps were constructed. The maxima of the response to the acoustic tones of different frequencies is indicated near the right y-axis. The centroid of each response map was computed as the means of the x and y co-ordinates (depth and post-stimulus time). Since the computation of the mean can be seriously skewed by low-level activity far from the main focus, the centroid were computed from map pixels in which the counts of the multi-unit activity were 50% of more of the maximum.

Histology

At the conclusion of the mapping study, the cat was transitioned to deep Nembutal anesthesia and perfused through the aorta with 1 L of phosphate-buffered saline followed by 1.5 L of 4% buffered formalin. The array's superstructure was then removed from the brainstem. During implantation of the array, the lateral part of the cerebellum had been aspirated and the void was replaced by loose connective tissue. In the process of dissecting the array cable from this tissue, all 4 of the silicon tines fractured from the epoxy superstructure and remained in the fixed tissue. (We are developing our own version of the silicon probes using the deep reactive ion etching process, which should preclude such fractures.) The cochlear nucleus was embedded into paraffin and sectioned in the frontal plane at 8 μm and the section stained with Cresyl violet. The presence of the fractured probe shanks in the tissue did cause some disruption of the tissue sections, but the anatomical locations of the 4 probes and the condition of the neurons and neuropil adjacent to the tracks could be determined.

RESULTS

In the past quarter, terminal experiments were conduced on two cat, cn149 at 439 days after array implantation and CN153, 253 days after implantation. In cat cn149, the array had rotated into a nearly horizontal position, apparently due to downward pressure from the cable, which extended dorsally from the array to the craniectomy. The orientation of the array in cat CN153 was essentially as when implanted, with the silicon shanks oriented in a nearly dorso-ventral direction, and thus approximately along the tonotopic gradient of the ventral nucleus. Thus the data from CN153 are more representative of the capabilities of a chronically-implanted microstimulating array.

A sketch of the entire array is shown in the inset at the bottom of figure. Figures 2a shows the upper part of the track of the caudal-lateral and nearly the entire track of the caudal-medial shanks passing into the posteroventral cochlear nucleus of cat CN153. The dorsolateral surface of the nucleus has been flattened by the array superstructure. The opaque entities are the shattered remnants of the silicon shanks. The PVCN is identified as the region of multipolar and spherical cells rostral of the octopus cell region, and

without a laminated structure (Osen, 1969) Figure 2b shows normal-appearing neurons and neuropil within 100 µm of the caudal-lateral shank. Figure 2c shows the tracks of the rostral-medial and rostral-lateral shanks, 1.5 m rostral of the caudal shanks, entering the ventral cochlear nucleus, caudal of the entry zone of the auditory nerve. Based on the cytoarchtecture, this appear to be the rostral part of the PVCN. Figure 2d shows neurons near the track of the rostral-lateral shank.

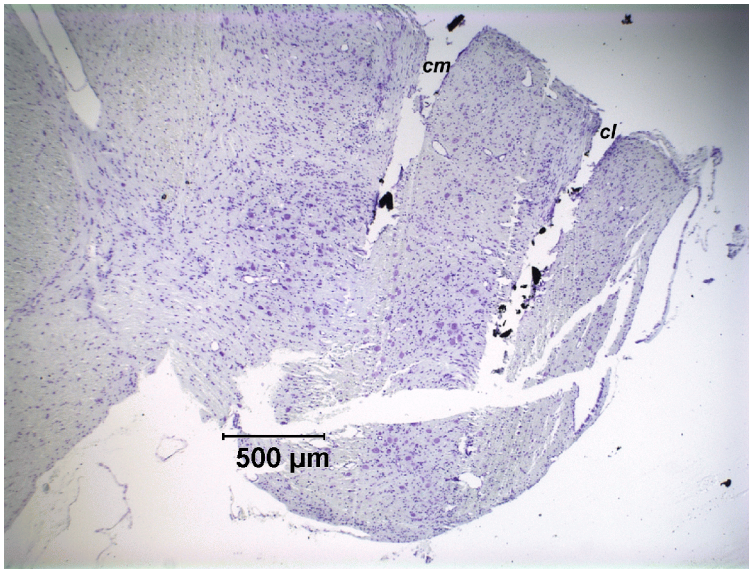

Figure 2A. Tracks of caudal shanks

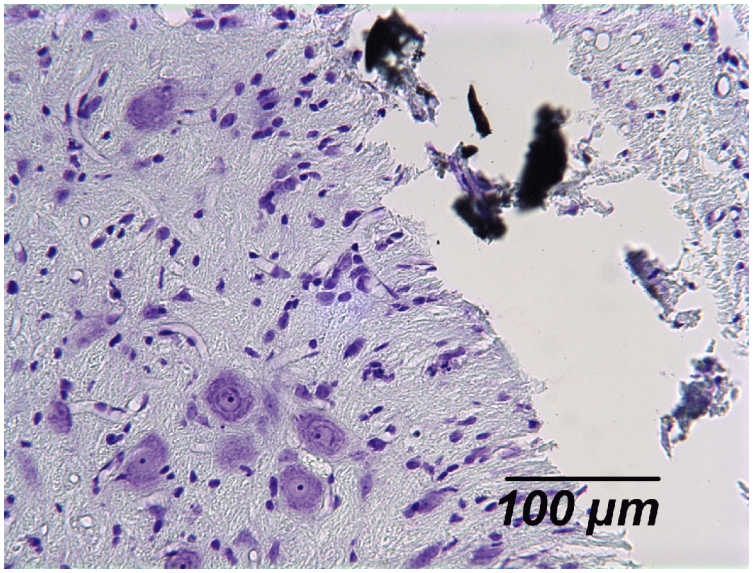

Figure 2B. Neurons near caudal-lateral shank

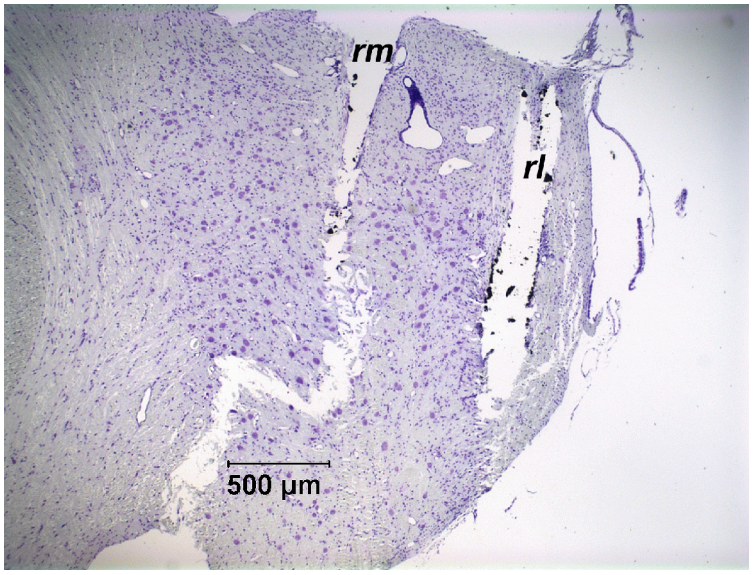

Figure 2C. Tracks of rostral shanks

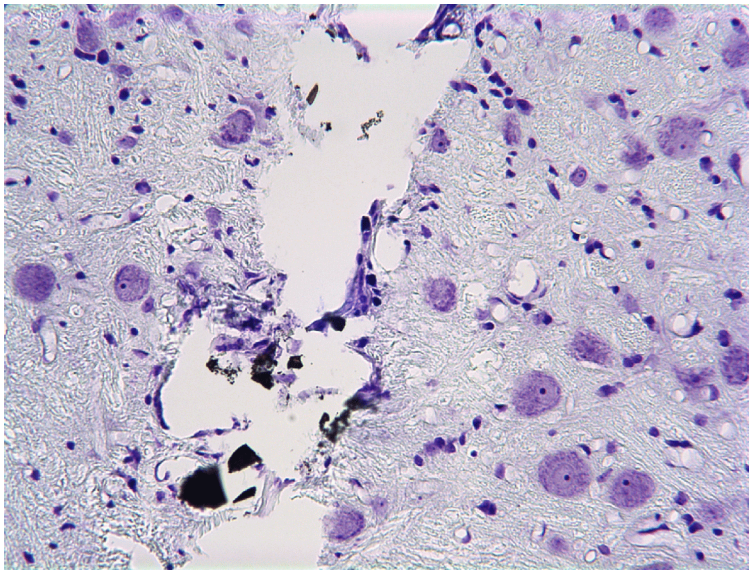

Figure 2d. Neurons near rostral-medial shank

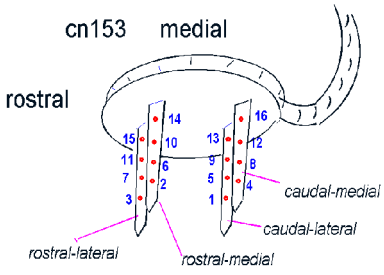

Figure 2. Tracks of silicon shanks in the ventral cochlear nucleus of cat CN153.

Figure 3A, B show the response growth functions (RGFs) recorded from cat CN153 at 22 and 250 days after implantation of the microstimulating array in the cochlear nucleus. Each frame shows the amplitude of the earliest component of the compound response evoked from the sites on a particular silicon shank in the CN, the locations of which are shown in the inset at the bottom of the figure.

Between the 22nd and 250th day after implantation, the threshold and slope of the RGFs were quite constant. The change in the relative slope and threshold of the responses from the various sites suggest some ongoing movement of the array through the tissue. At autopsy, the array's superstructure was seen to have depressed the dorsolateral surface of the cochlear nucleus by about 0.5 mm. As noted previously, this may be related to the small but continuous downward force exerted by the silicon encapsulated cable, which in the cat model is routed dorsally from the array, up to its attachment on the bone at the edge of the craniectomy. Silicone elastomer does absorb water *in vivo,* and tends to expand, causing the cable to lengthen slightly. We have revised the cable design to include a dog leg segment that should absorb the downward force as the cable lengthens slightly.

22 days	250 days
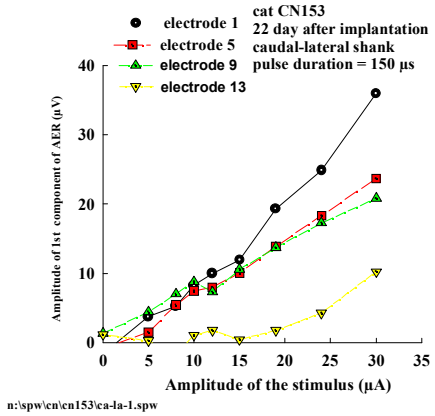	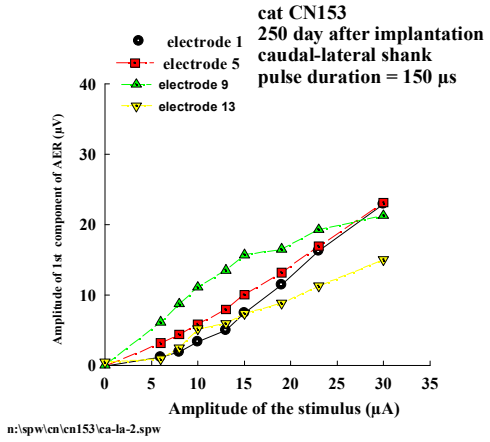
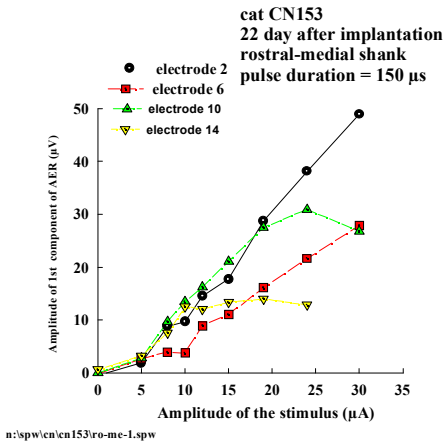	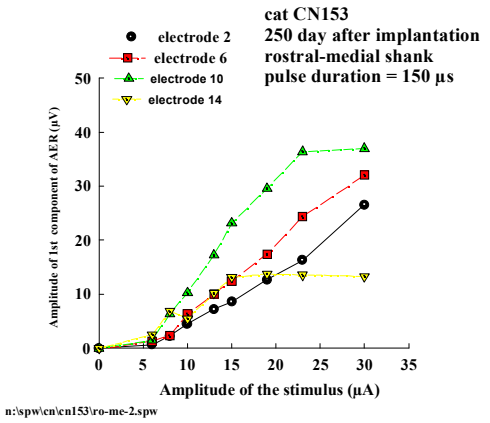
Figure 3A. Response growth functions from cat CN153, recorded at 22 and 250 days after implantation of the stimulating array	

22 days

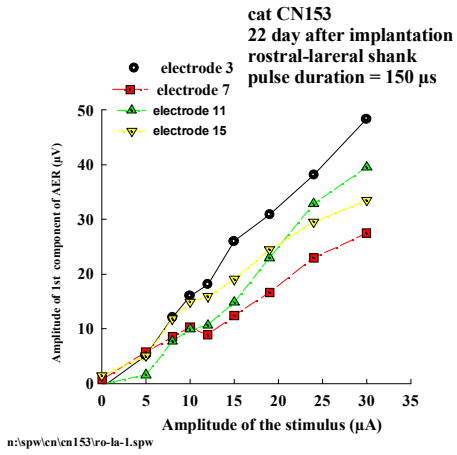

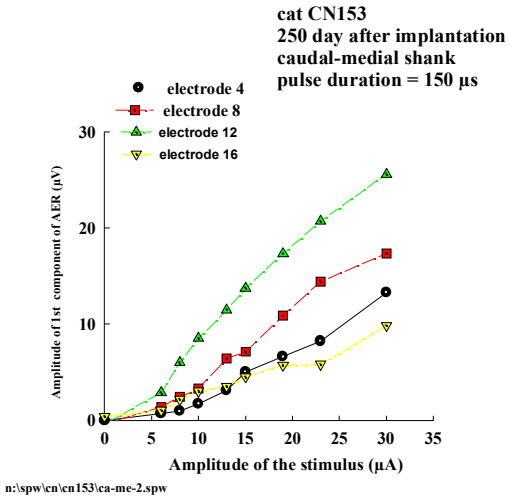

250 days

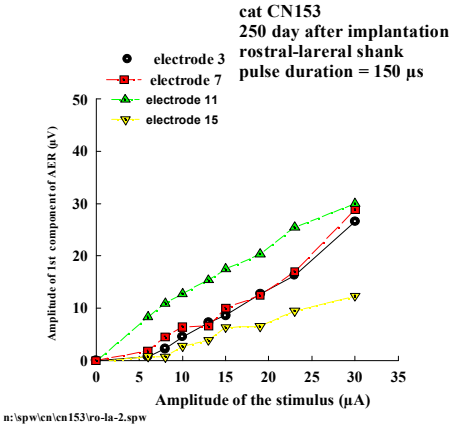

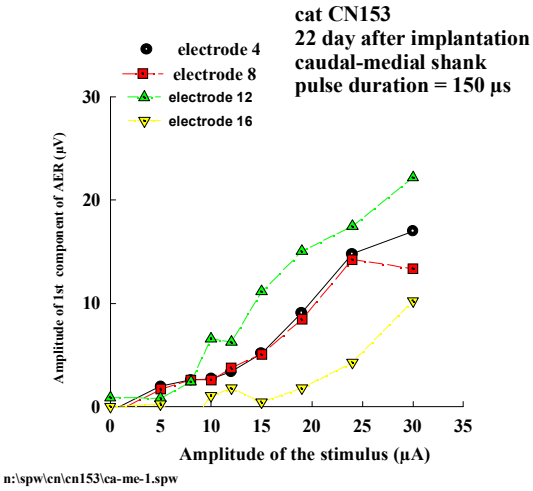

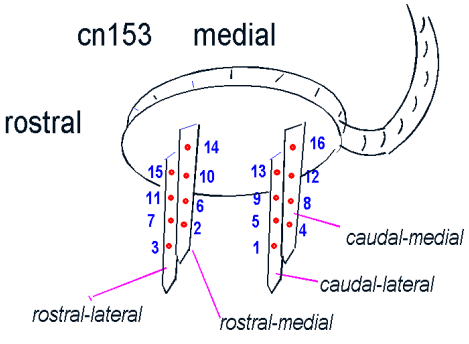

Figure 3B

Frequency response maps recorded in the central nucleus of the inferior colliculus.

In the terminal experiment of cat 153, the 32-site recording probes was inserted into the IC at three locations. Penetration 1 was rostral and the entry point was lateral in the IC, above the brachium of the inferior colliculus. Penetrations 2 and 3 were more caudal, about midway along the rostral-caudal extent of the central nucleus. The point of entry of penetration 2 on the dorsal surface of the IC was medial and that of penetration 3 was lateral

Figure 4A, B, C show the response maps recorded during penetration 1 into the central nucleus of the inferior colliculus while stimulating in the contralateral cochlear nucleus at 10, 20 or 30 μA. In each map, the abscissa is the time after the start of the stimulus pulse, and the left-hand ordinate is the distance from the tip of the 32-site recording probe. The response maxima to acoustic tone bursts of various frequencies are plotted on the right ordinate. The map contour lines correspond to the iso-response contours, in units of the number of action potential in each of the 100 μs bins of the PST histograms from which the maps are constructed. Particularly at the lowest stimulus amplitude, (10 μA) some of the maps did not contain a focus of multiunit activity, and this condition is designated as "no focus." In each panel, each column represents the responses from the sites on one of the silicon shanks in the CN, and the rows correspond to the stimulating sites on the shanks, with the response maps from the deepest sites in the CN at the top of the panel and the responses from the shallower sites at the bottom. In penetration 1, the response foci spanned a depth range greater than the 3-mm span of the recording sites, so in a second run, the recording probe was advanced an additional 1 mm into the IC along the same track, and response evoked by the shallowest stimulating sites in the CN was again recorded (Figure 4D, E, F). The response maps from penetrations 2 and 3 in the IC are shown in Figs. 5 & 6, respectively. Note that the response thresholds of most of the sites were slightly higher in penetration 3, which the entered the IC from its mediolateral surface.

The depth coordinate of the centroid of the activity evoked in the IC are plotted as bars in Figure 7, for each stimulating site in the CN and for each of the 3 penetrations into the IC. The range brackets for each bar are the standard deviation of the span in depth of the activity focus, and provide an index of the dispersion over depth in the ICC of the neuronal activity evoked from each site in the CN and the overlap of the activity evoked from adjacent sites. The maps of penetration 1 were acquired with the tip of the recording probe at two different depths, and the left-hand ordinate is with respect to the shallower penetration. For the caudal-lateral and caudal-medial shanks, the centroids progress regularly from deep to shallow in the IC as the site of the microstimulation moves from shallow to deep in the PVCN. This progression is seen most clearly in the data from penetration 3. Each of the sites on the caudal-medial shank evoked responses deeper in the IC (corresponding to higher acoustic frequencies) than the corresponding site on the caudal-lateral shank. This is as expected, since the array was inserted into the dorsolateral wall of the cochlear nucleus, and thus would be expected to traverse the isofrequency lamina of the PVCN at an oblique angle (Quarterly Progress Reports #4 & #5). Together, the 8 sites on the caudal shanks in the PVCN spanned a range of acoustic frequencies from greater than 25 KHz to approximately 1 KHz. For the 2 rostral shanks, the regular progression of the centroids from deep to shallow in the IC was seen only for penetration 3. In penetration 1, the response maps from stimulating site 1 on the rostral-lateral shank was distributed over a range of depths in the IC. Similarly, in penetration 2, the response map for stimulating site 7 on the rostral-lateral shank, and for site 2 and 6 on the rostral-medial shank, were distributed over a range of depths in the IC (Figure 4). There are two possible explanations for this. The distribution of the response evoked from a particular site in the CN would be recorded over a larger range of depths in the IC if we were recording action potentials from axons projecting out of the central nucleus and also from their cells of origin in a particular isofrequency lamina in the IC. A second possibility is that some of the stimulating sites on the rostral shanks were exciting neurons representing a wider range of acoustic frequencies. Since the thresholds and depth spans of the activity foci varied for the different penetrations into the ICC, this explanation also imply that the neural activity evoked from a particular location in the CN does not project uniformly to all parts of an particular isofrequency lamina in the ICC.

DISCUSSION

The results described above illustrate the capacity of a microstimulating array implanted chronically in

the feline cochlear nucleus to access the tonotopic gradient of the ventral cochlear nucleus. The human and feline ventral cochlear nuclei contain similar cell types, and the nuclei of both species are of similar size and architecture, so these data demonstrate the potential for a central auditory prosthesis using multisite silicon substrate probes. The findings also suggest the number and density of shanks and individual stimulating sites on each shank that will be necessary to access the entire tonotopic gradient of the human CN. Figure 6 illustrates how the stimulating sites on each of the two caudal shanks in the caudal part posteroventral cochlear nucleus work in synergy with the sites on the adjacent shank to provide access to 8 distinctive locations along the tonotopic gradient of the ventral nucleus, while also spanning a wide range of acoustic frequencies. The sites on the rostral shanks contribute additional points of access to the tonotopic gradient. However, the response maps indicate that the neuronal activity induced by these sites is spread over a greater part of the tonotopic gradient.

The findings described in this and previous reports convey only a rudamentary description of the capacity of a high-density microstimulating array to convey information into the central auditory system. What is most needed is a multisite, multishank recording probe that can be implanted chronically into the inferior colliculus, with a linear span greater than the dorso-ventral span of the ICC. This will allow comprehensive studies using a variety of stimulus frequencies, amplitudes and temporal patterns, with the animal unanesthetized or more likely, very lightly anesthetized. We currently have such a probe under development. In view of previous studies by other investigators that have suggested the inhomogeneity of the isofrequency lamina of the ICC, our own findings suggesting the same are not surprising, but they do complicate the problem of implanting a chronic recording probe into the feline ICC, since only the most rostral part of the IC (e.g, penetration 1 in this study) extends beyond the rostral edge of the ossified tentorium. Thus the entry point for penetrations 2 and 3 in the present study required removal of part of the tentorium, which will be difficult in animals designated for long-term survival.

caudal-lateral shank	rostral-medial	rostral-lateral	caudal-medial
electrode 1 no focus	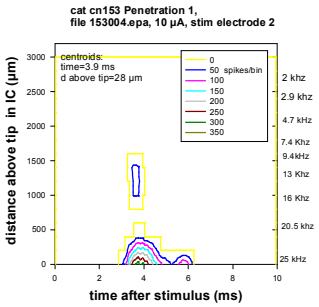	electrode 3 no focus	electrode 4 no focus
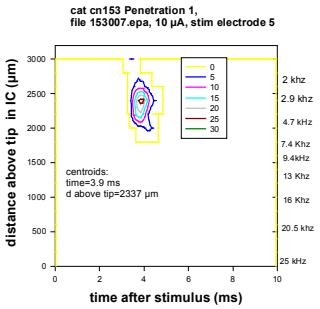	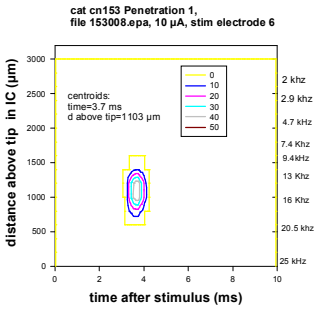	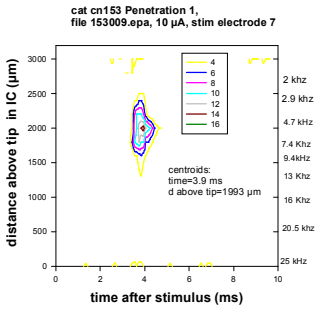	electrode 8 no focus
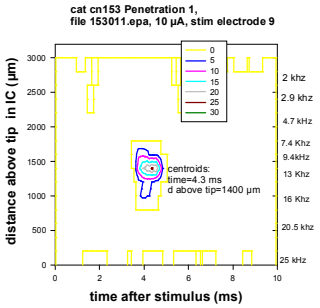	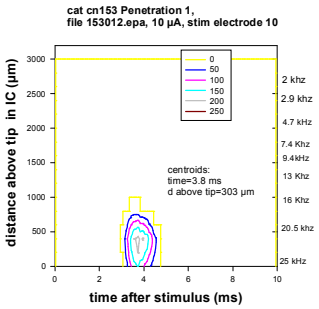	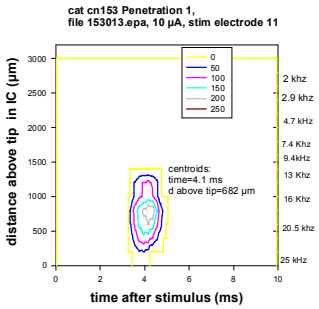	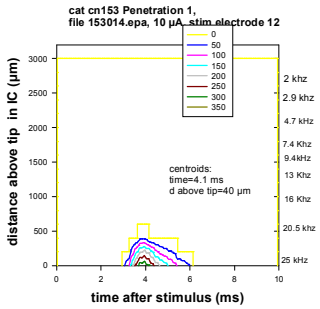
electrode 13 no focus	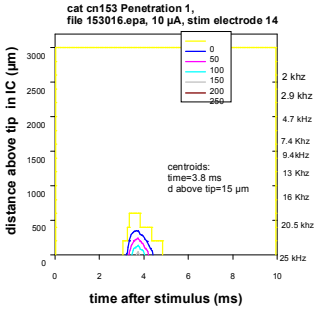	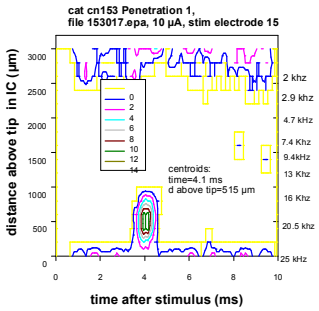	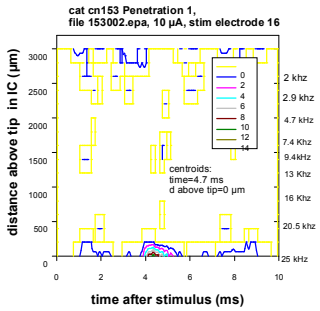

Figure 4A. Penetration 1 into the IC, stimulus = 10 µA. (point of entry of recording electrode in rostral-lateral IC)

caudal-lateral	rostral-medial	rostral-lateral	caudal-medial
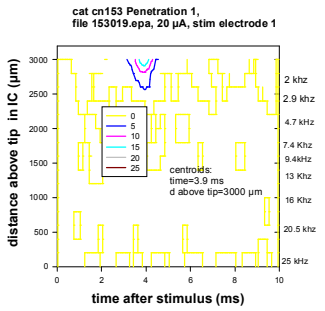	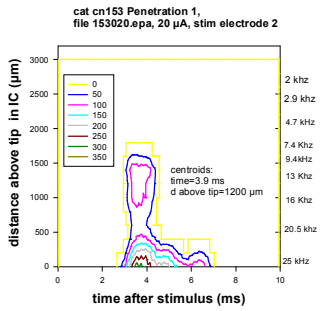	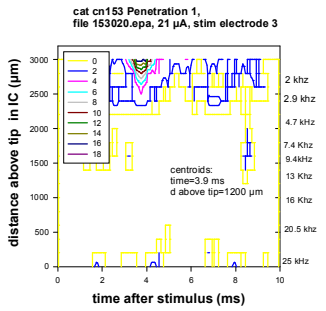	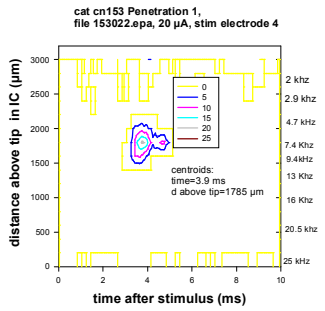
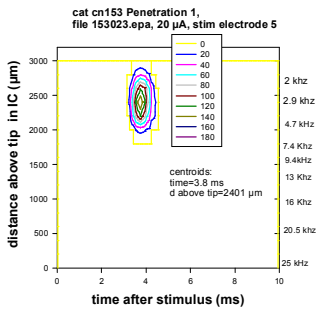	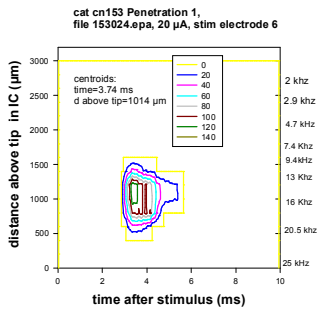	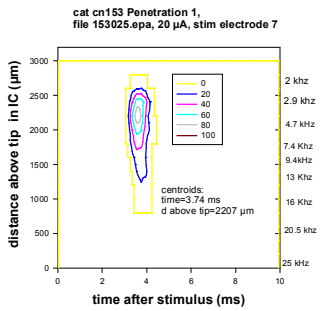	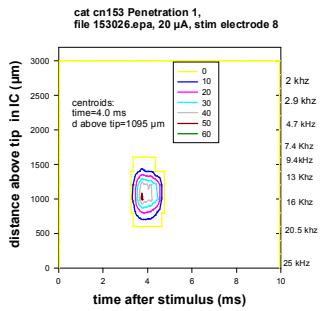
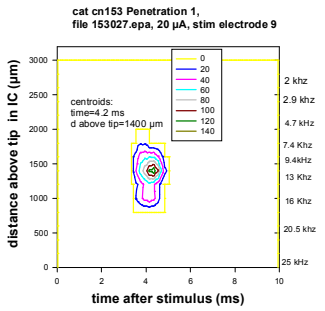	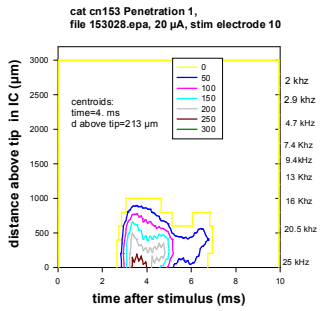	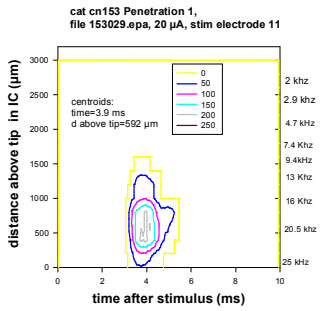	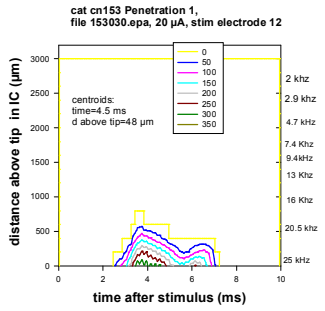
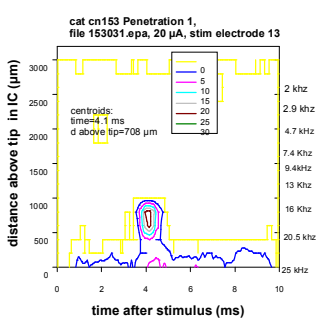	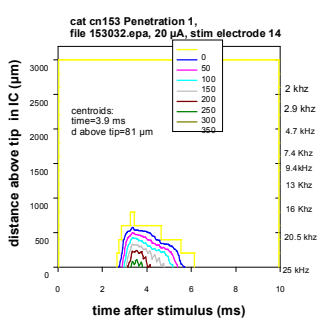	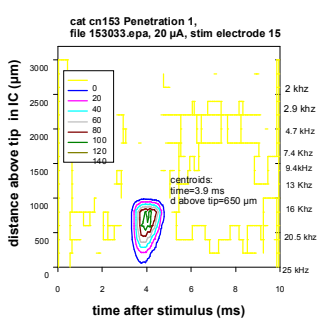	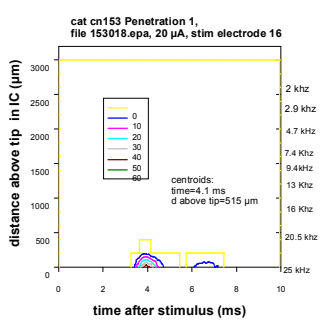

Figure 4B . Penetration 1, stimulus= 20 µA

caudal-lateral shank	rostral-medial	rostral-lateral	caudal-medial
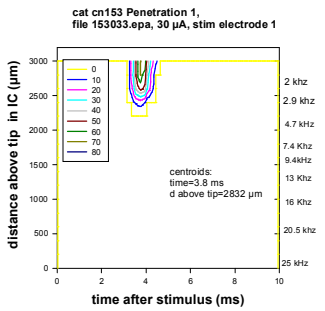	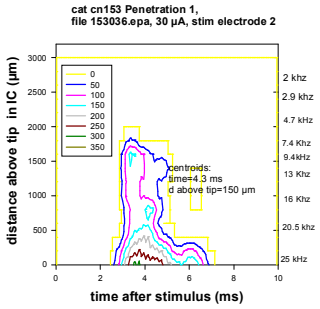	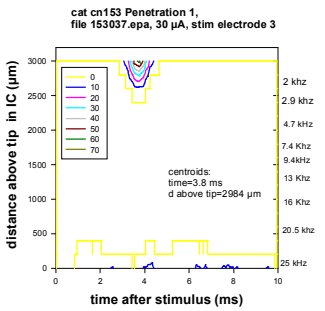	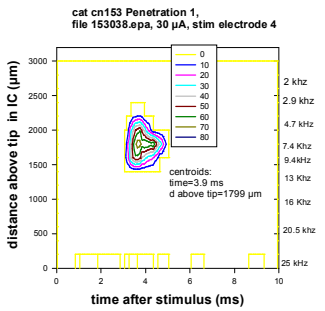
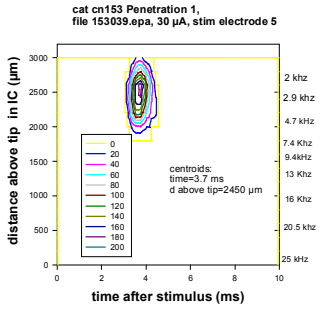	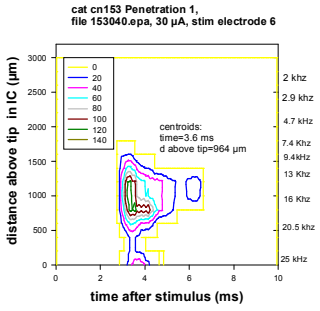	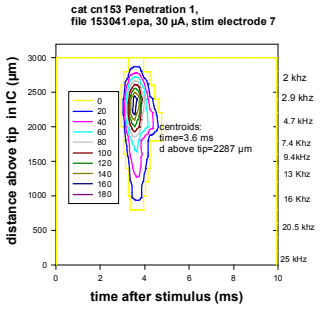	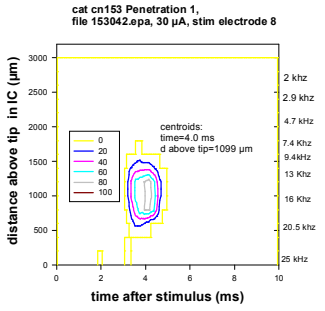
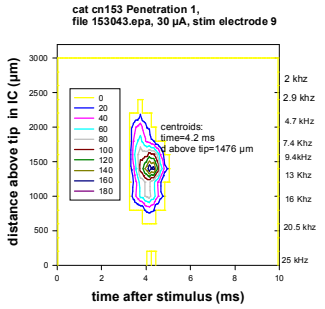	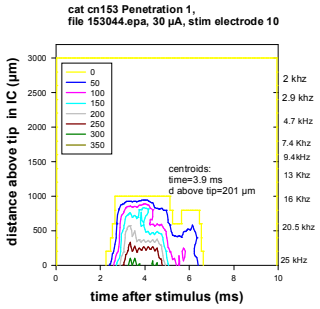	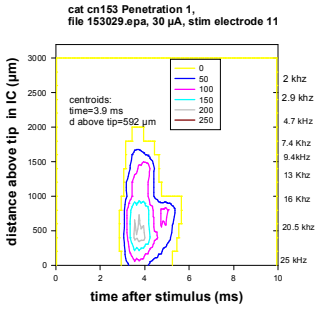	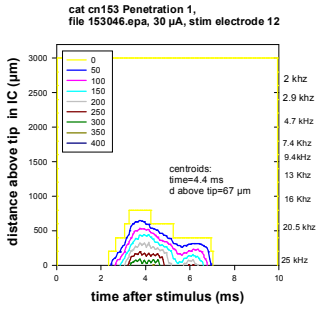
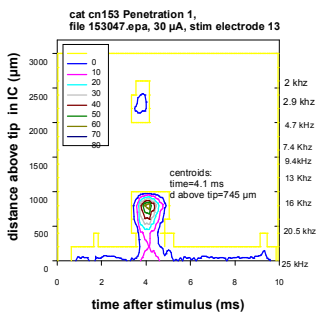	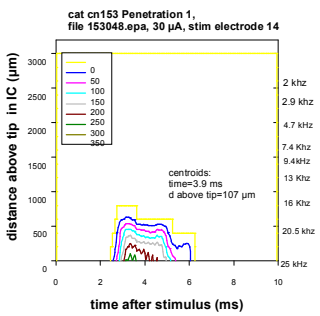	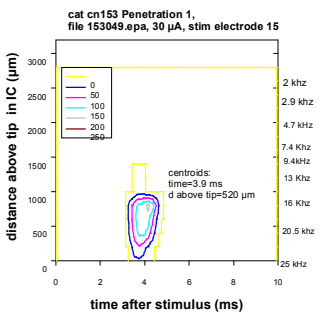	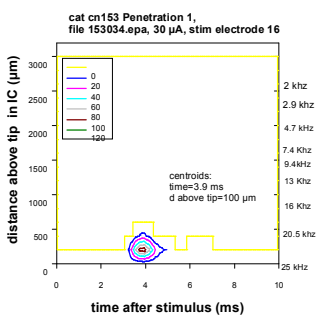

Figure 4C. Penetration 1, stimulus = 30 µA.

caudal-lateral shank	rostral-medial	rostral-lateral	caudal-medial
Not acquired	not acquired	not acquired	not acquired
not acquired	not acquired	not acquired	not acquired
not acquired	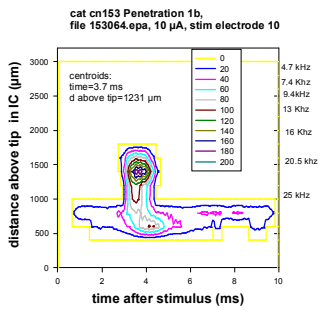	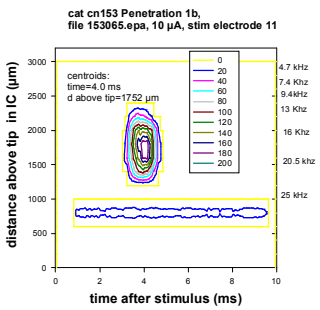	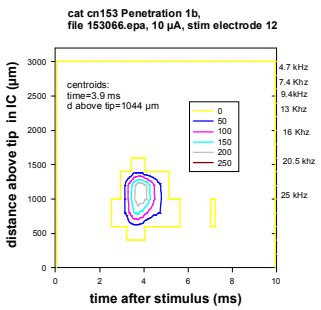
Electrode 13 No focus	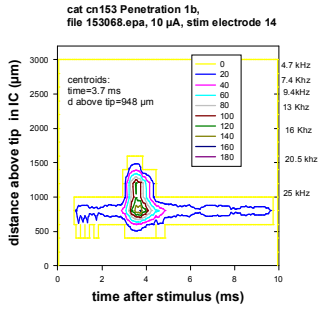	electrode 15 No focus	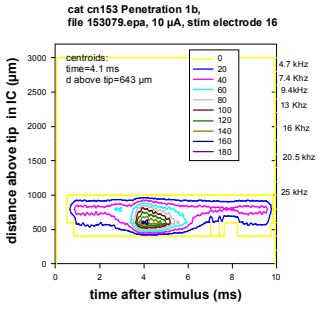

Figure 4D. stimulus = 10 µA (Still penetration 1, but tip of recording electrode 1 mm deeper in the IC)

caudal-lateral shank	rostral-medial	rostral-lateral	caudal-medial
not acquired	not acquired	not acquired	nota acquired
not acquired	nota acquired	not acquired	nota acquired
not acquired	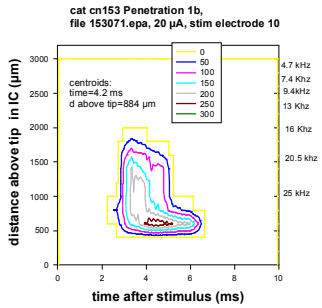	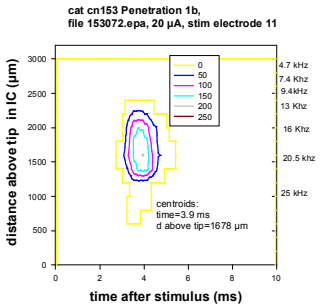	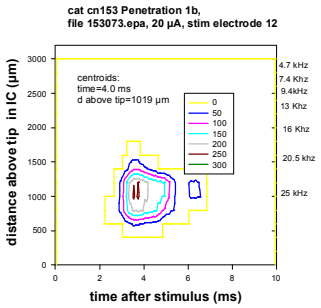
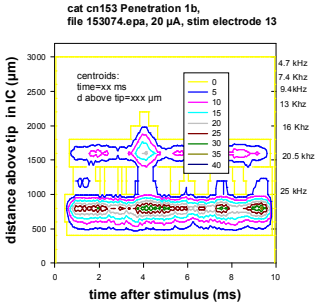	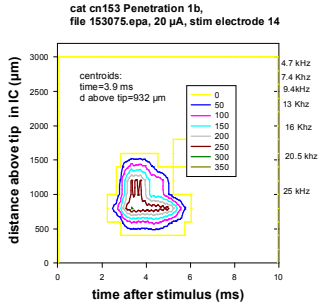	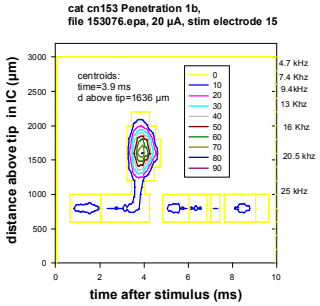	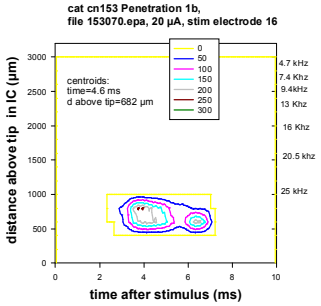

Figure 4E, stimulus = 20 µA

caudal-lateral	rostral-medial	rostral-lateral	caudal-medial
not acquired	not acquired	not acquired	not acquired
not acquired	not acquired	nota acquired	not acquired
not acquired	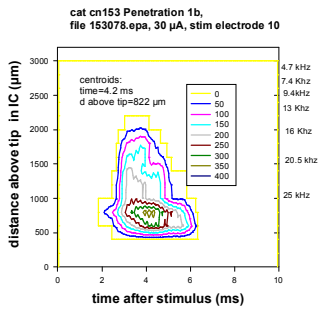	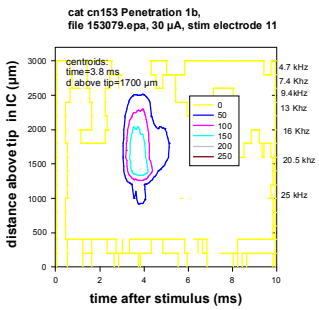	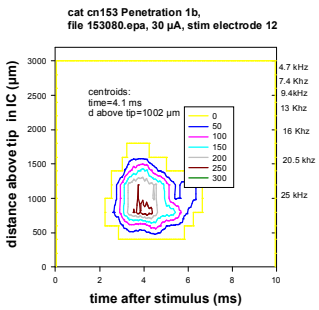
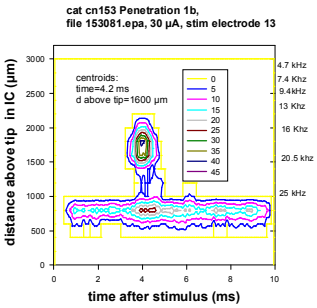	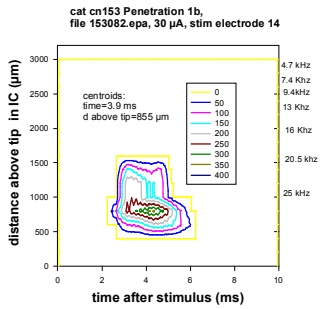	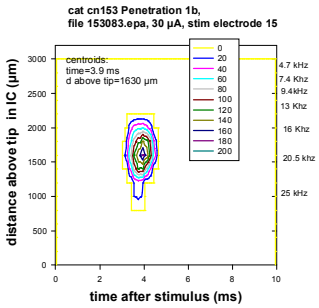	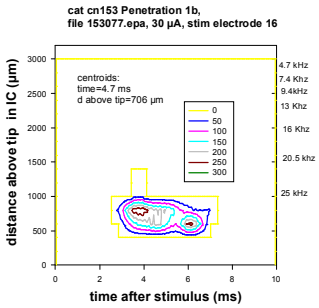

Figure 4F, stimulus= 30 µA

caudal-lateral shank	rostral-medial	rostral-lateral	caudal-medial
Electrode 1 no focus	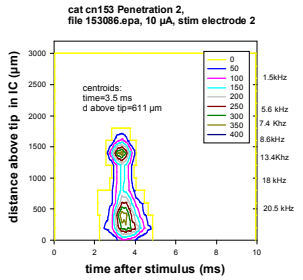	electrode 3 no focus	electrode 4 no focus
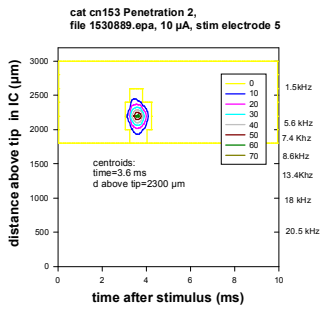	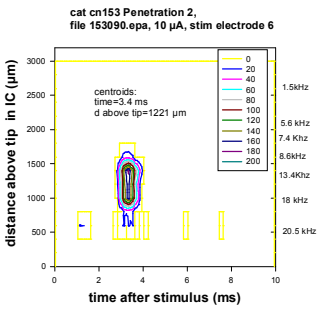	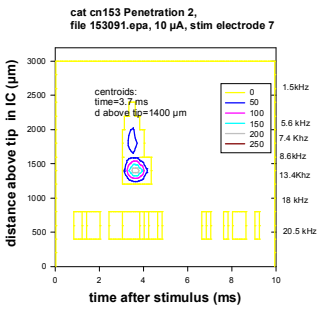	electrode 8 no focus
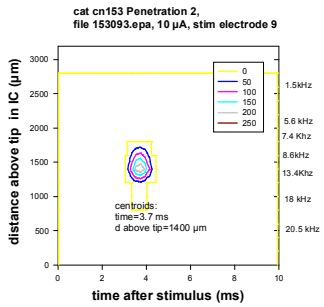	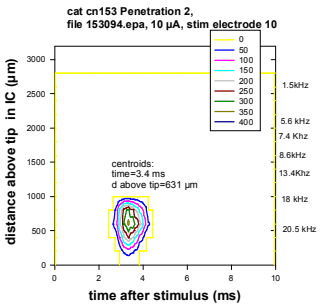	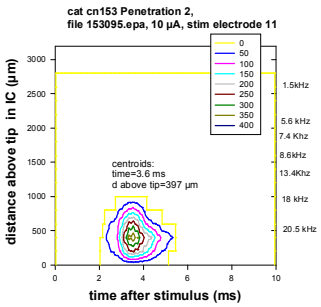	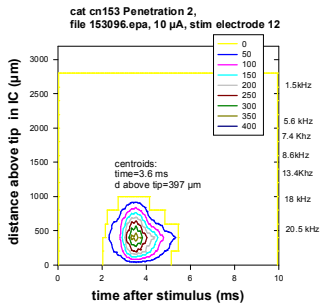
electrode 13 no focus of activity	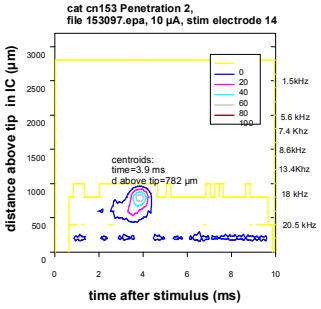	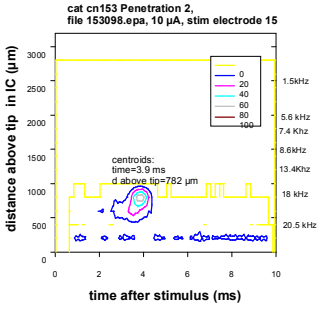	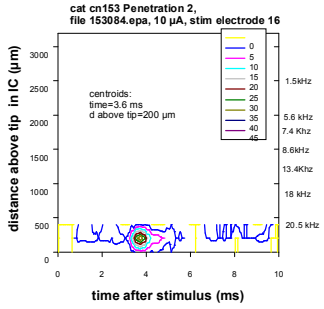

Figure 5A, Penetration 2. stimulus =10 µA (Point of entry of recording electrode in medial-medial IC)

caudal-lateral shank	rostral-medial	rostral-lateral	caudal-medial
electrode 1 no focus	electrode 2 no focus	electrode 3 no focus	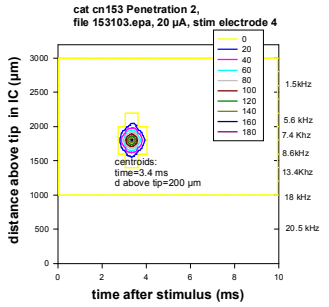
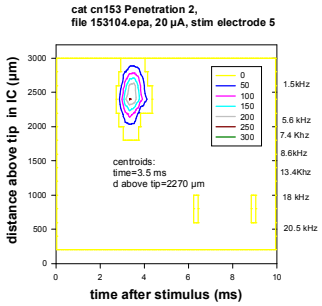	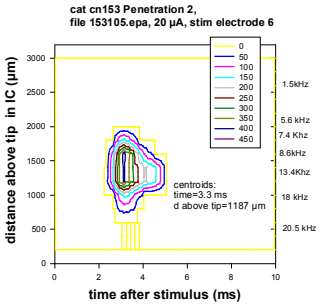	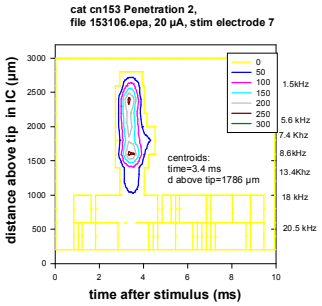	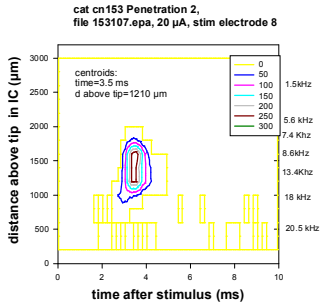
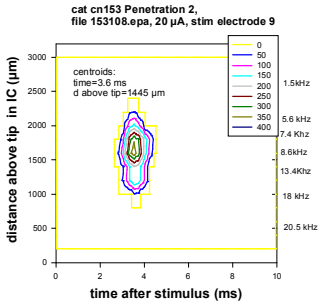	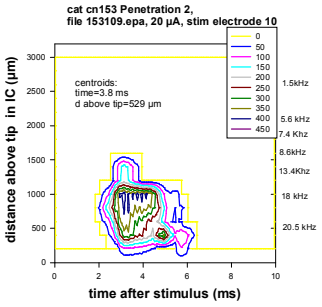	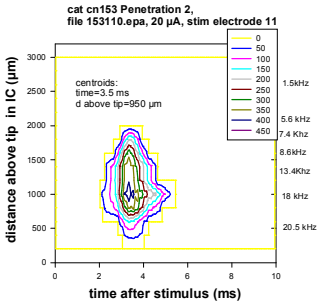	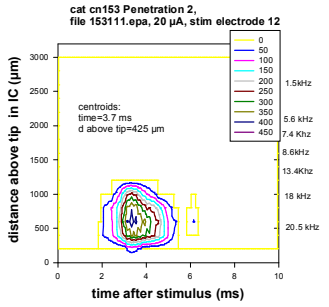
electrode 13 no focus of activity	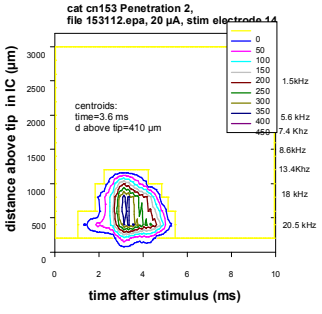	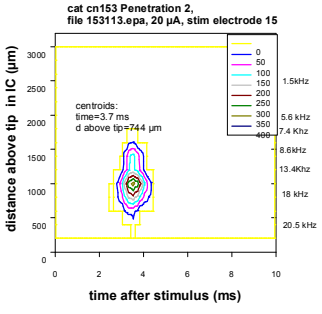	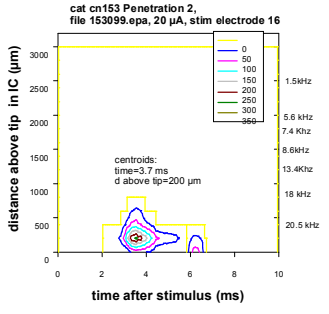

Figure 5B, Penetration 2. stimulus=20 µA

caudal-lateral	rostral-medial	rostral-lateral	caudal-medial
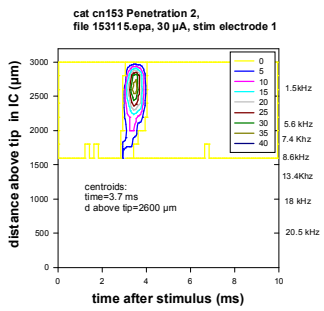	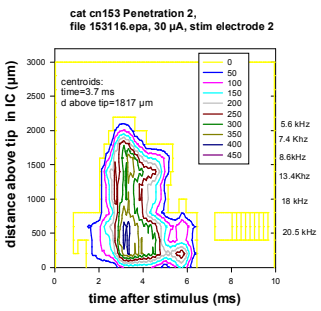	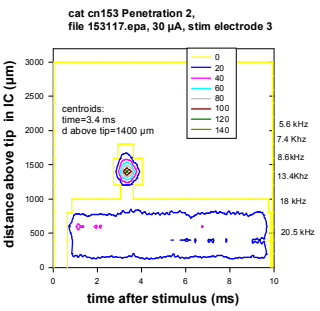	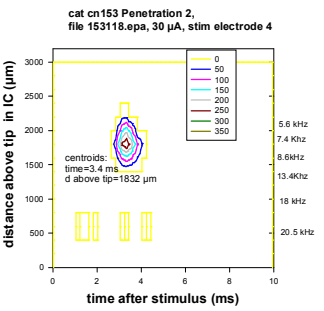
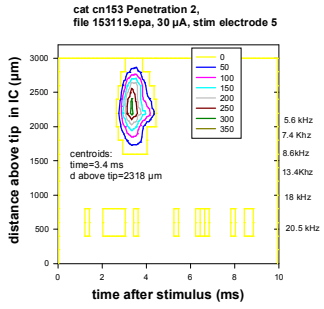	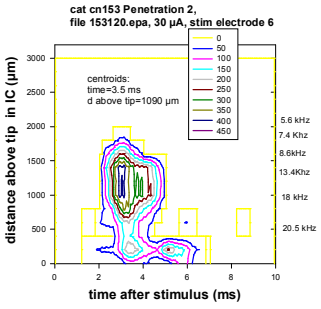	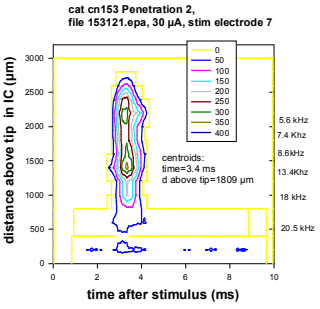	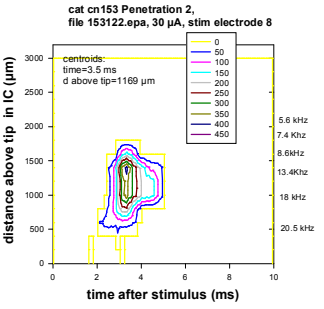
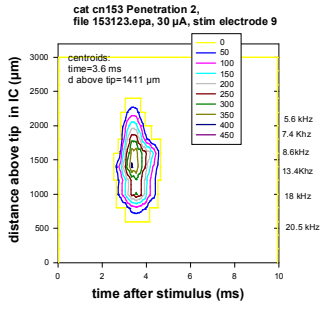	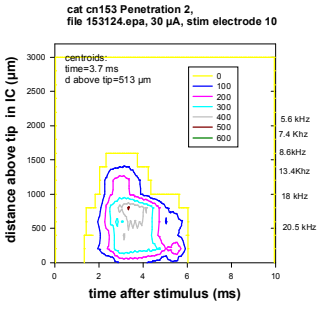	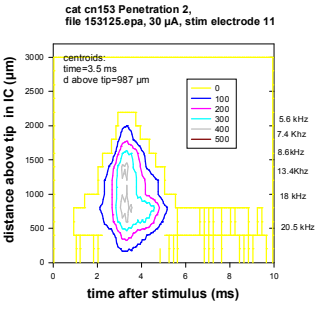	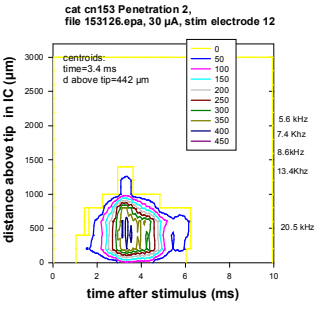
no focus of activity	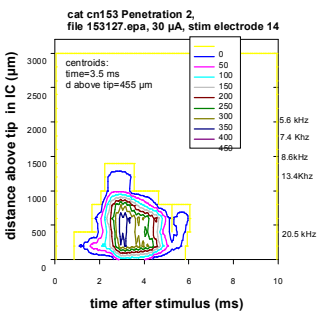	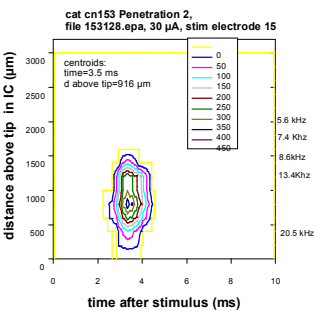	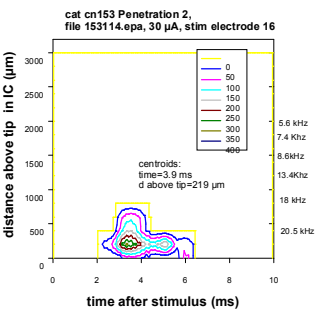

Figure 5C, Penetration 2, stimulus=30 µA

Caudal-lateral shank	rostral-medial	rostral-lateral	caudal-medial
electrode 1 No focus of activity	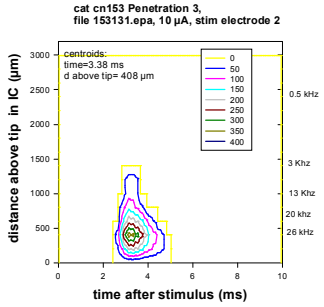	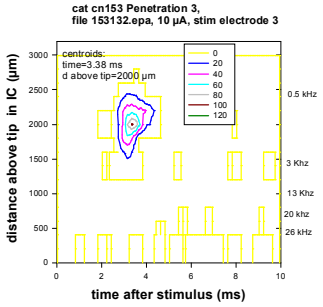	electrode 4 no focus of activity
electrode 5 No focus	electrode 6 no focus	electrode 7 no focus	electrode 8 no focus
electrode 9 no focus	electrode 10 no focus	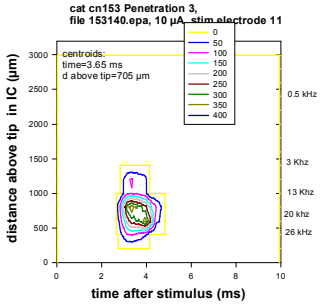	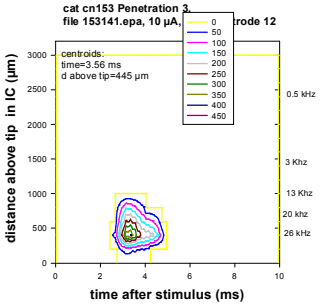
electrodes 13 no focus	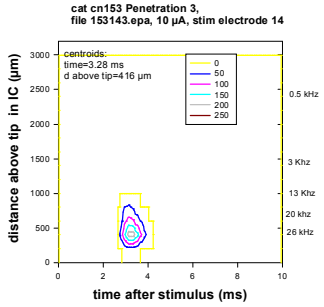	electrode 15 no focus	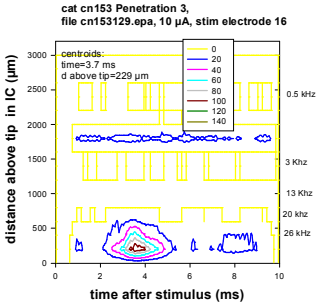

Figure 6A, Penetration 3, stimulus = 10 µA (recording electrodes entered medial-lateral IC)

caudal-lateral shank	rostral-medial shank	rostral-lateral	caudal-medial
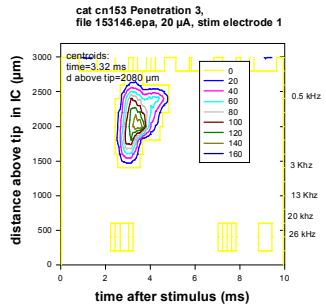	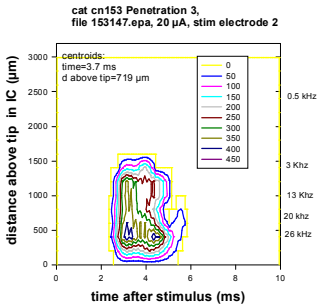	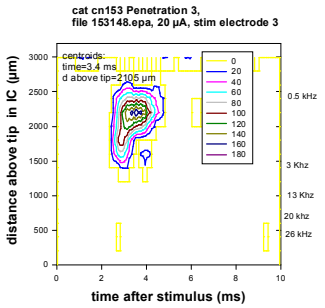	Electrode 4 no focus
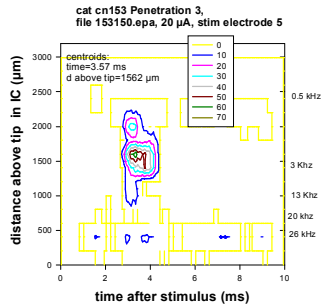	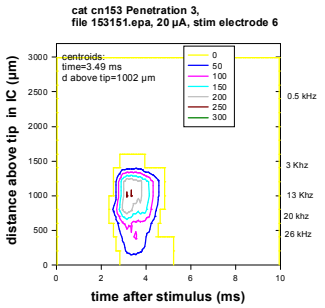	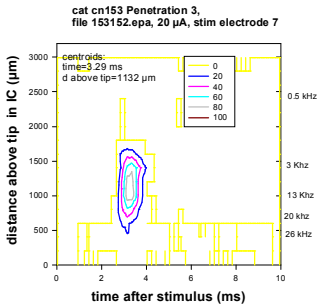	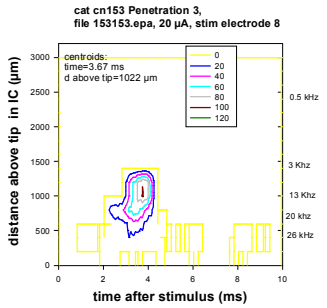
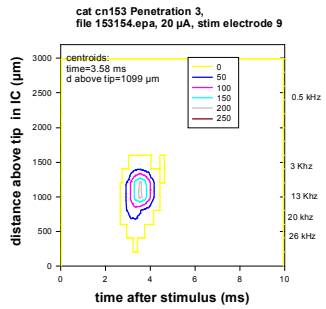	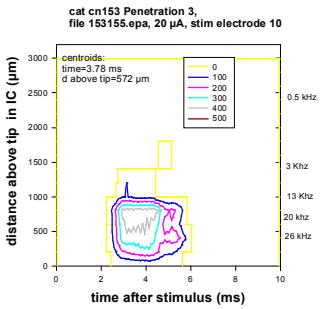	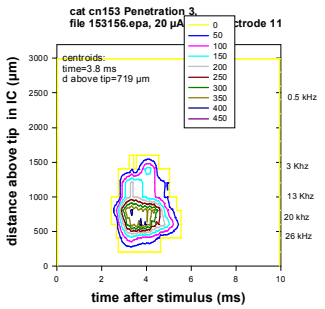	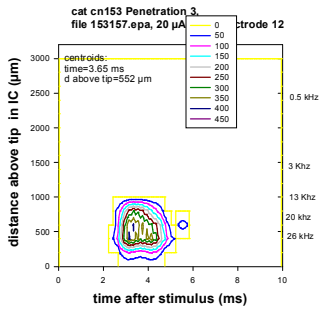
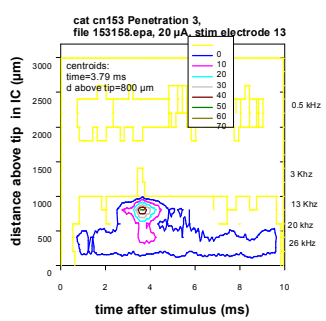	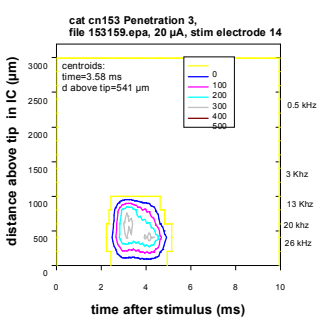	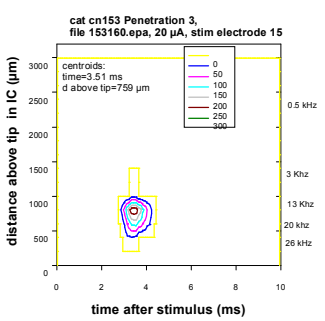	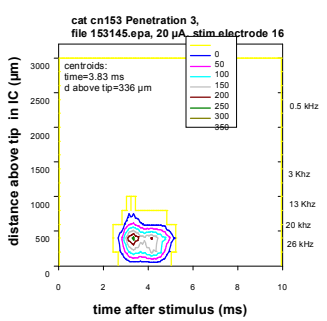

Figure 6B, penetration 3, 20 µA

caudal-lateral	rostral -medial	rostral-lateral	caudal-medial
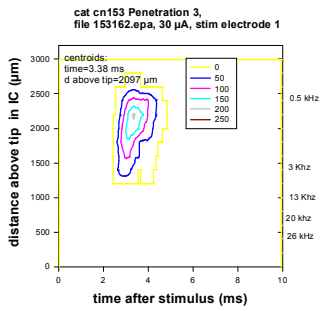	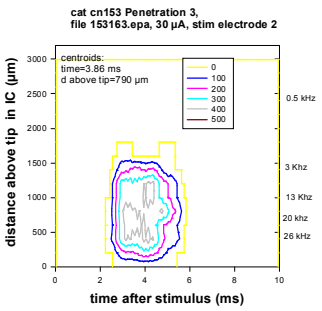	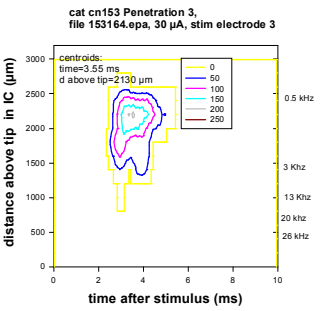	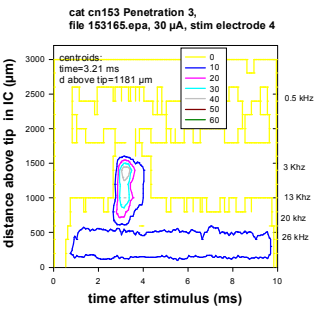
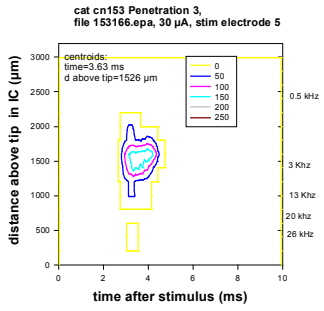	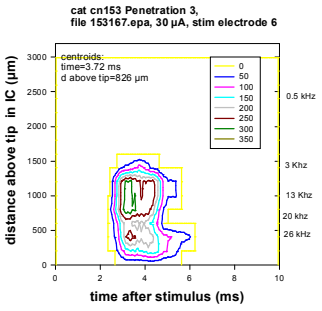	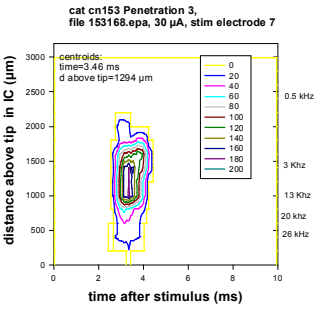	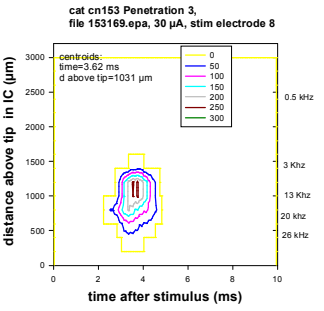
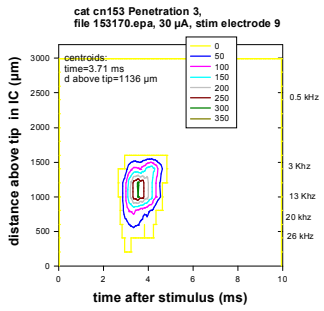	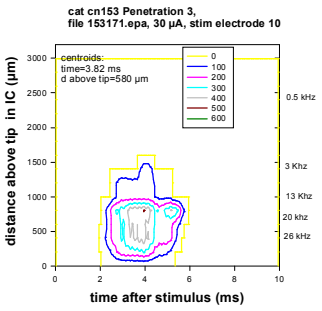	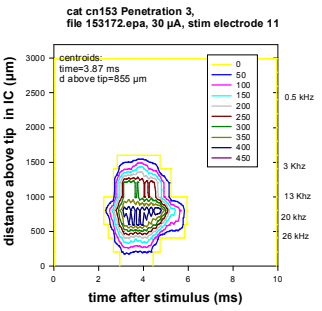	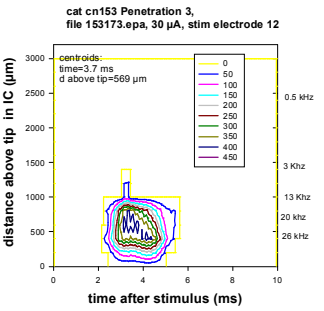
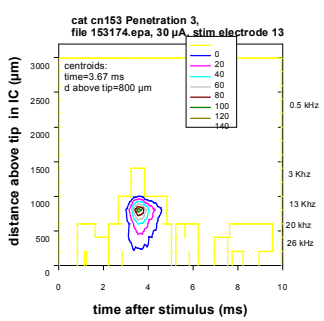	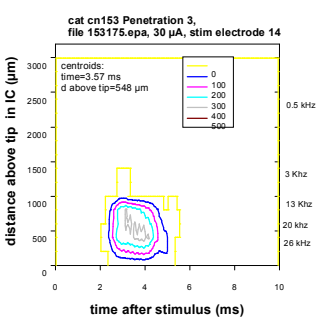	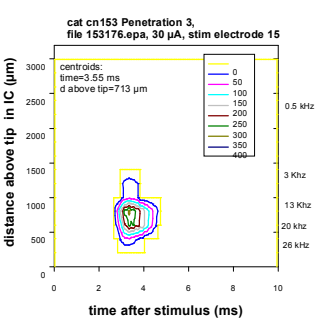	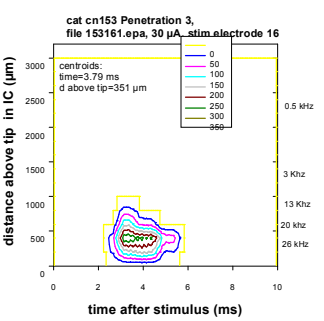

Figure 6C, penetration 3, stimulus= 30 µA

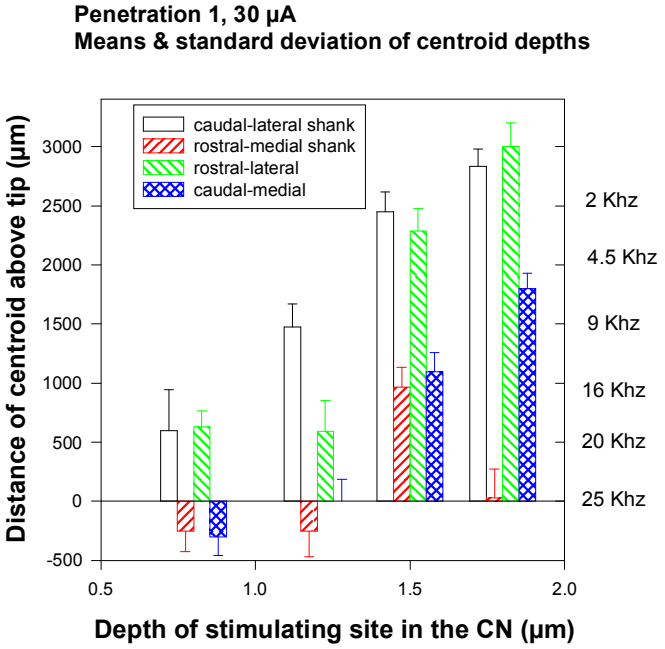

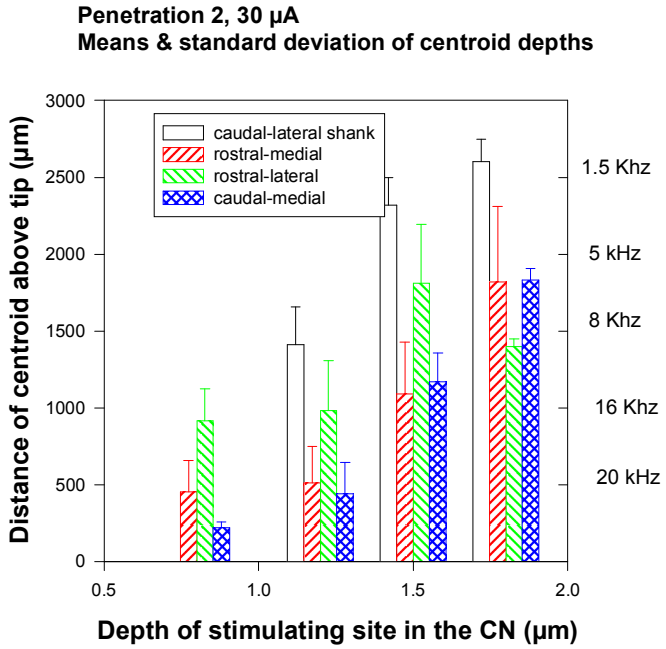

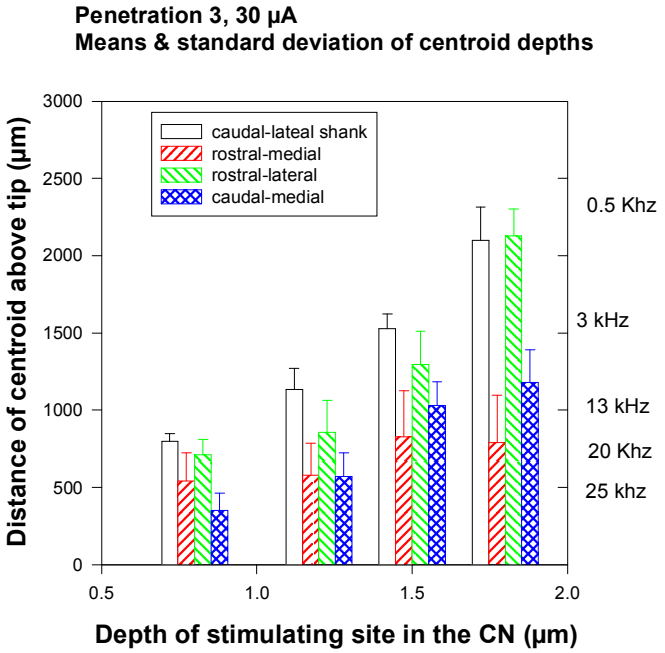

Figure 7. CAT CN153. The locations of the centroids of the maps of multi-unit activity in the IC evoked from each of the stimulating sites in the CN (bars) and the standard deviation of the span of the activity above and below the centroid (range brackets), for each of the 3 penetrations into the IC

2: Summary of work completed at the House Ear Institute

On Dec 13, 2005, the 6th patient was implanted with an array of macroelectrodes in the lateral recess and the array of penetrating microelectrodes. This hybrid implant is designated the penetrating ABI (PABI). PABI patient #6 received the new revised model of the penetrating array with 10 stimulating sites, each with increased surface area (8,000 μm^2) to allow use of a greater charge range. The implant's device was activated on Jan 15, 2006. The patient was unable to use the surface array due to intolerable non-auditory side effects but 6 of the microelectrodes on the penetrating array produced auditory percepts over a full range of loudness without side effects. Data from this patient will be presented in the next quarterly report.

Testing of patients in Verona, Italy

In a testing session in December 2005,data were obtained on temporal integration and thresholds as a function of pulse phase duration from 9 patients with the surface type of auditory brains implants (ABI's). The first patient with a surface ABI device placed on the Inferior Colliculus (called the Inferior Colliculus Implant - ICI) also was tested. For most of these patients, their deafness was of etiologies other than Type 2 Neurofibromatosis (NF2) and some had high levels of speech recognition with the ABI. Testing focused on temporal measures on the hypothesis that speech recognition and temporal resolution were linked. Previous test results show a significant correlation between speech recognition and temporal modulation detection levels (Fu et al., 2002; Colletti and Shannon, 2005).

Temporal integration measured threshold levels as a function of the duration of the stimulus burst.

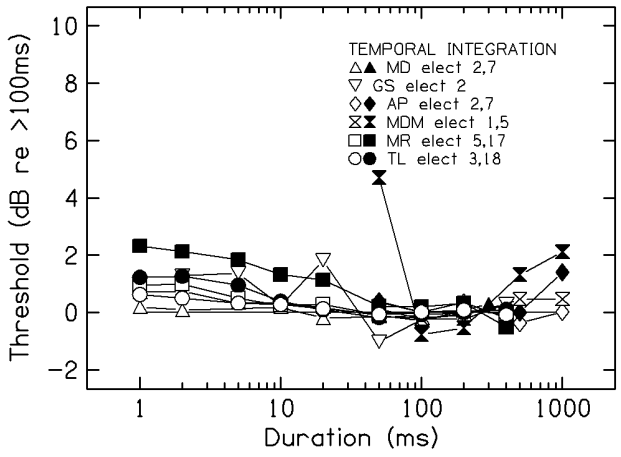

Figure 8

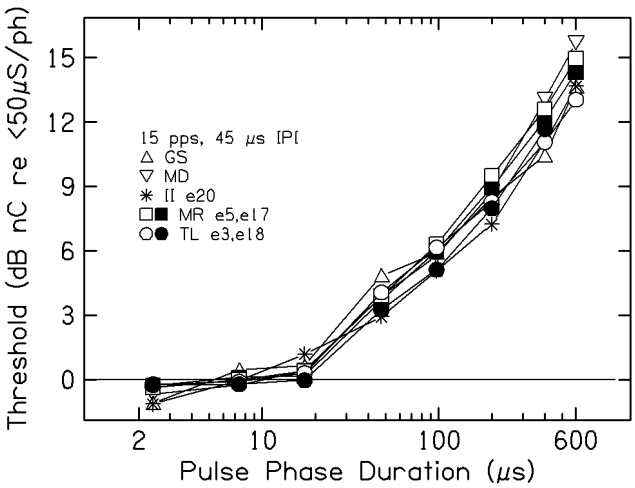

Figure 9

Temporal integration measures the trade-off between stimulus level at threshold and the length of the burst. If energy was integrated perfectly over the duration of stimulation, then a burst that was twice as long would require a stimulation level with half of the energy. The temporal integration function shows the time constant and magnitude of this trade off. Stimulation rate was set at 1000 pps and thresholds were measured for bursts ranging from 1 ms to 1000 ms duration. Results from six non-NF2 ABI patients presented in Figure 8 show little change in threshold as a function of burst duration. For most patients thresholds only increased by 1.5-2 dB as burst duration was decreased from 100 ms to 1 ms (single biphasic pulse). This result is similar to the lack of temporal integration observed in cochlear implant and ABI patients with NF2. Previous models (Shannon, 1990) suggest that the lack of temporal integration is due to the fact that the integration occurs at a perceptual level, i.e. twice as much "perceptual energy" is necessary to compensate for a stimulus that is half as long. But due to the expansive nature of the loudness mapping function for electrical stimulation, only a small amount of electrical current increase is necessary to double the perceived loudness. Thus, although there is a trade-off between perceived magnitude and stimulation duration, when

plotted in terms of dB at the input, threshold rises only slightly in terms of dB as stimulus duration is shortened.

Threshold levels as a function of pulse phase duration may indicate the size and type of neurons activated by the electrical stimulation. Electrically, neurons have a specific capacitance derived from their cross sectional diameter (conductive fluid surrounded by insulating myelin). Threshold charge per phase will decrease with decreasing pulse phase duration until the combined phases are shorter than the time constant of the cell membrane, at which point the second phase is able to cancel electrical charge still held by the membrane. Axons typically have shorter time constants (50-100 μs) than cell bodies (200μs-10 ms). One possibility for the difference in performance between NF2 and non-tumor ABI patients is in the differential survival of large vs small cells in the cochlear nucleus. We measured threshold as a function of pulse phase duration for a low pulse rate (15 pps)in five non-tumor ABI patients. The separation of phases in each biphasic pulse (inter phase interval: IPI) was 45 us. Figure 9 shows that threshold decreases with phase duration down to 20 us, suggesting that the ABI was activating small fibers rather than dendrites or cell bodies. Similar measures will be made for NF2 ABI patients, CI patients for comparison, and for patients with electrodes on the Inferior Colliculus (ICI), both surface and penetrating. This comparison may show a difference in the effective time constant which would indicate differential survival of selective nerve types in the CN following NF2 tumor removal. The comparison with CI and ICI should give us an idea of how sensitive this measure is. Presumably cochlear implants stimulate a mix of dendritic peripheral processes of the auditory nerve as well as cell bodies in the spiral ganglion, while ICI electrodes would activate a mix of cell types in the IC. It is not clear at present if this measure is sensitive enough to differentiate between NF2 and non-tumor ABI patients. The data in Figure 9 suggest activation of axons. If NF2 results show a significantly longer time constant it might indicate activation of cell bodies directly.

Work in the Next Quarter (Jan-Feb-Mar 2006)

In the next quarter of this contract we anticipate implantation of 3-4 additional PABI patients. Modifications have been made to the penetrating electrode to add two additional stimulating points by ablating insulation from the stabilizing pins at 2.5 mm from the base.

REFERENCES

Colletti V and Shannon RV (2005). Open Set Speech Perception with Auditory Brainstem Implant? The Laryngoscope 115:1974-1978.

Fu, Q.-J. (2002). Temporal processing and speech recognition in cochlear implant users, NeuroReport, 13: 1635-1639.

Shannon, R.V. (1990). A model of temporal integration and forward masking for electrical stimulation of the auditory nerve, in Models of the Electrically stimulated Cochlea, J.M. Miller and F.A. Spelman (Eds.), Springer-Verlag, New York, pp. 187-205.